Journal of Ceramic Processing Research. Vol. 16, Special. 1, pp. 74s~82s (2015)

J O U R N A L O F
Ceramic Processing Research

Mechanical behavior of a capsule embedded in cementitious matrix-macro model and numerical simulation

X.F. Wang[a], F. Xing[a,*], Q. Xie[a], N.X. Han[a], T. Kishi[b] and T.H. Ahn[c]

[a]*Guangdong Provincial Key Laboratory of Durability for Marine Civil Engineering, College of Civil Engineering, Shenzhen University, Shenzhen, P.R. China*

[b]*Department of Human & Social System, Institute of Industrial Science, The University of Tokyo, 4-6-1, Komaba, Meguro-Ku, Tokyo, 153-8505, Japan.*

[c]*International Sustainable Engineering Materials (ISEM) Center, Ceramic Materials Institute & Division of Advanced Materials Sci. Eng. Hanyang University, Seoul 133-791 Korea*

The self-healing cementitious composites by using microcapsules have been developed in Guangdong Provincial Key Laboratory of Durability for Marine Civil Engineering. The diameters of the microcapsules were located from tens to several hundred micro meters. Since it is usually difficult to measure the stress distribution and the fracture behavior in detail on this microscope scale, in this study, macro capsule model experiments were designed to simulate the behavior of a micro-capsule embedded in cementitious materials. Then, numerical analysis was conducted to study the interaction between a crack and a microcapsule. A criterion for judgment of the failure pattern: rupture or debonding of a microcapsule was obtained.

Key words: Microcapsules, Crack, Self-healing, Mechanical behavior, Numerical simulation.

Introduction

It is known that reinforced concrete structures suffer from deterioration under circumstance and loading conditions with ages. This may cause durability problems. Usually, they are treated by using afterward repairing method, such as grouting or plaster casting method. However, continuous inspection and maintenance should be difficult to implement when damages are not visible or accessible. Since the pioneer work on self-healing materials by White *et al* (2001) was published, as a new strategy to achieve performance recovery of materials or structures, it has attracted more and more researchers' attention. In 2013, a total over 200 papers were presented in 4th international conference on self-healing materials (Proceedings ICSHM 2013) which was normally biannually opened [18, 23]. Also, there have been several review papers published in recent years. de Rooij *et al.* (2013), Joseph *et al*. (2010), Wu *et al*. (2012), Tittelboom & Belie (2013), and Mihashi and Nishiwaki (2012) presented reviews on self-healing in cementitious materials and engineered cementitious composite as a self-healing material [4, 11, 21, 24].

JCI Technical Committee on Autogenous Healing in Cementitious Materials [7] proposed a kind of classification of phenomena and definitions of terms on self-healing/repairing concrete, which included (1) natural healing; (2) autonomic healing; and (3) activated repairing. It was also indicated that autogenous healing encompassed natural healing and autonomic healing; Engineered healing/repairing covered autonomic healing and activated repairing; and self-healing/repairing encompassed the whole phenomenon of closing of cracks in concrete not by human hand.

RILEM Technical Committee 221-SHC [4] proposed a set of evolved definitions by using the terms "autogenic" and "autonomic", in which "autogenic" represented the recovery process using materials components that belong to own generic materials, and "autonomic" indicated the recovery process using materials components that are engineered additions which would not be found in the original material. Self-healing represented any process by the materials involving the performance recovery.

Mihashi and Nishiwaki (2012) proposed a classification of two groups, one, called "engineered self-healing", focused on the potential retaining capability in cementitious composites to fill cracks. It was subdivided into two sub-groups: natural self-healing and engineered self-healing. The other is called "self-repairing", in which cracks can be repaired functionally by some devices embedded in advance for that purpose. It was also subdivided into two sub-groups: passive mode and active mode self-repairing.

Wang *et al*. (2013) suggested that the schemes of self-healing materials developed could be divided to two levels.. One was at the material level, such as by using bacteria [9, 10, 20], microcapsules [26, 22], or

*Corresponding author:
Tel : +86 -755 -2653-4021
Fax: +86 -755 -2653-4021
E-mail: xingf@szu.edu.cn

expansive agents and mineral admixtures [2, 13], and the other was at the structural level, which included approaches by hollow glass fibers [5, 6, 14, 16, 17], shape memory alloy or polymer *et al*. [8, 19]. The former is usually in passive mode, though sensors like devices are being developed at present. The latter usually can be designed in active and/or smart mode.

Microcapsules, as temporary vessels, hold healing agent till damage induced trigger occurs. It is efficient and has special benefit from durability point of view. Although the method needs to be further developed and be investigated in future, encapsulation scheme looks to be a promising approach to self-healing.

From 2008, various types of self-healing cementitious composites by using organic and inorganic microcapsules have been developed in Guangdong Provincial Key Laboratory of Durability for Marine Civil Engineering [22, 26]. In their study, it was found that the integrity of microcapsules was maintained during the making of the cement paste, and the microcapsules ruptured when cracks passed through them. The pictures of the organic microcapsules under normal scale and optical microscopy are shown in Figure 1. Figure 2 shows a specimen of self-healing cementitious materials containing microcapsules. The effect of various proportions of microcapsules was also investigated. In Figure 3, the results of the orthogonal experiments show the variation of recovery rates with microcapsule contents for both flexural and compression strength, in which the recovery rate was defined as follows [22]:

$$\text{recevery rate} = \frac{\text{strength after healing}}{\text{original strength}} \times 100\% \qquad (1)$$

The results showed that the recovery rates increased almost linearly with increasing the microcapsule contents. This could provide a definite proof of validation for this approach, which meant that macro mechanical properties could be indeed recovered in a self-healing sense. Though a positive result has been earned for the macro behavior, it is essential to investigate the detail of its mechanism which involves rupture or debonding of a single microcapsule. The diameters of the microcapsules are located from tens to several hundred micro meters. Since it is usually difficult to measure the stress distribution and the fracture behavior in detail on this microscope scale, in this study, macro capsule model experiments were designed to simulate the behavior of a microcapsule embedded in cementitious materials. Also, numerical analysis was conducted to study the interaction between a crack and a microcapsule with the parameters being

(a) Under normal scale

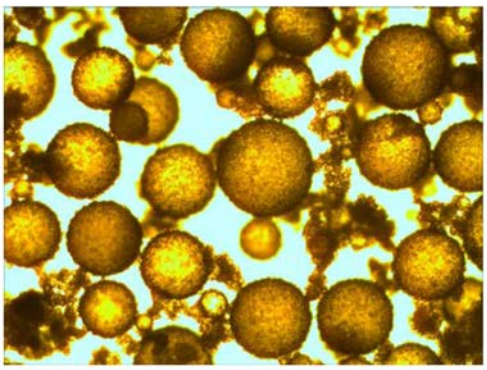

(b) Under optical microscopy

Fig. 1. A kind of organic microcapsules.

Fig. 2. A specimen of microcapsule based self-healing cementitious materials.

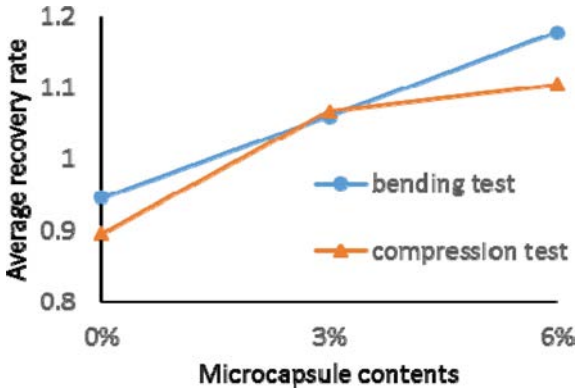

Fig. 3. Variation of strength recovery rate for the specimens with different microcapsule contents.

Fig. 4. Simulating macro capsules.

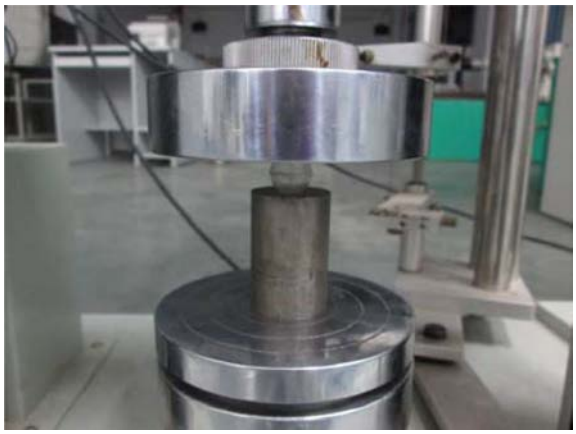

Fig. 5. Experimental set up for compression of a capsule.

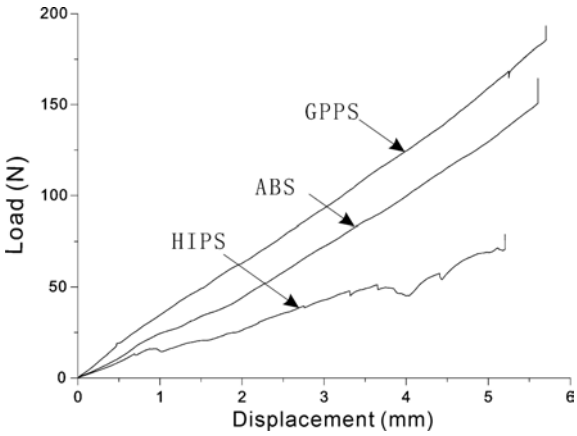

Fig. 6. Compression of capsules.

location of crack, microcapsule shell thickness, strength of microcapsule shell, and the debonding strength of the interface between microcapsule and mortar matrix. A criterion for judgment of a microcapsule's rupture or debonding was obtained.

Experiments and Discussions

Macro capsules

To investigate the effect of wall material of capsules and to simulate the behavior of microcapsules, 3 types of macro capsules of different wall materials (GPPS, ABS, HIPS) were selected. The raw materials were from Kumho Petrochemical Co. Ltd. Table 1 lists the properties of density, tensile strength, flexural strength, and flexural modulus for the three raw materials, as well as urea-formaldehyde (UF) [3], which was used for the wall material of organic microcapsules. It is seen that except density, UF has similar properties with the analogue materials.

Table 1. Properties of three types of capsules.

Capsule type	Density (g/cm^3)	Tensile strength (kg/cm^2)	Flexural Strength (kg/cm^2)	Flexural modulus (kg/cm^2)
Urea-formaldehyde	1.4-1.5	410-920	700-1120	
GPPS-GP150	1.04	550	900	35000
ABS-BM150	1.04	430	620	22000
HIPS-MIB237	1.03	250	380	19000

Figure 4 gives a picture of the simulating macro capsules, inside which was air. The size parameters were measured then. The average diameters of the three types of capsules were 15 mm. The thickness of capsule walls was measured in such way that, first zero degree longitude and zero degree latitude were determined, next from these two lines, the thickness at 0, 45, 90, 135, and 180 degrees was measured 15 times for each type of capsule for each direction, then the average values were obtained, t = 0.35 mm, 0.36 mm and 0.43 mm for GPPS, ABS, and HIPS capsules, respectively.

To determine the mechanical behavior of the capsules, compression tests were carried out. The testing machine was REGER-RWT10 (REGER Corp., Shenzhen, China). The experimental set up for compression of a capsule is shown in Figure 5. During the test, first, manually moved down the loading head, and stopped at the position about to come into contact with the capsule, (e.g. 1 mm by the naked eye). Then used the control software installed in the computer to set the loading head down the pressure with rate being 0.3 mm/min, in which the parameters were set to: starting point was 0.3 N, meanwhile the load and the displacement were cleared; the starting point for fracture was 10 N; the test would stop when the force value was less than 30%.

Figure 6 shows the load-displacement curves for the 3 types of capsules (GPPS, ABS, and HIPS). It was seen that the curves were almost linear, in which GPPS was the strongest, ABS was located in the center, and HIPS was the weakest. The curve for HIPS seems not very regular. This may due to its brittleness. From the characteristics of the curves stopping right after the ultimate loading points, it could be indicated that, basically, the three types of materials should be quite brittle. From the figure, it could be seen that the limiting loads were 185 N, 150 N and 70 N, for the capsules of GPPS, ABS, and HIPS, respectively. The indentation depths for all capsules were about 5-6 mm,

Fig. 7. Compression test of a mortar specimen with a capsule.

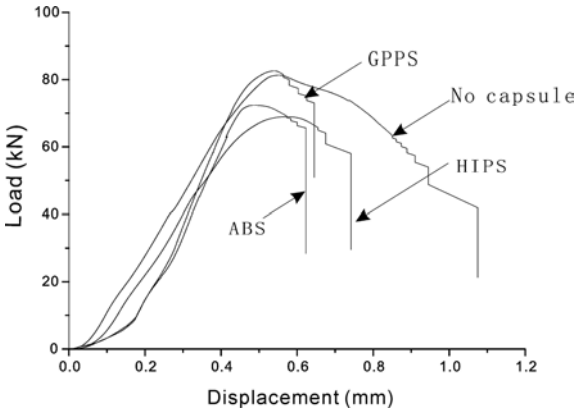

Fig. 8. Load-displacement curves in compression tests.

of which the ductility were very closed. In general, the material parameters such as young's modulus, Poisson ratio and some nonlinear parameters can be calibrated using these compression tests. Keller and Sottos (2006) determined the parameters using membrane theory model based on isotropic and linear elastic constitutive relationship hypothesis [12]. This meant the bending resistance of the capsule shell wall was neglected. However, for a general case, it should be a process of nonlinear optimization procedure, which needs further study in future.

Compression test of specimens

To investigate the self-healing mechanism of microcapsules, it necessary to understand the behavior of a capsule embedded in cementitious composite. To simulate this, first, compression tests for the specimens with a macro capsule inside each were carried out.

Cement mortar prismatic specimens of $40 \times 40 \times 160$ mm^3 were prepared, in which water cement ratio is 0.5; cement sand ratio was 1 : 3 in each specimen. Three types of capsules were set at the center of the specimens. The specimens were cured 28 days under standard condition. Reger-100 testing machine was used. The experimental set up is shown in Figure 7. The area under compression for each specimen was 40 mm × 40 mm. When the load was being exerted,

(a) Ruptured HIPS capsule in a compressed specimen

(b) ABS capsule remained intact in a compressed specimen

(c) GPPS capsule remained intact in a compressed specimen

Fig. 9. Morphology of a compressed specimen with a capsule.

similar to the previous section, used the control software to set the loading head down the pressure with rate being 0.5 mm/min.

The load-displacement curves for compression test of specimens with a capsule (GPPS, ABS, HIPS) and no capsule are shown in Figure 8. It can be seen that, basically, the strengths of specimens for GPPS capsule and no capsule were very similar (about 82 kN), The compressive strength for ABS and HIPS capsule specimens were 72 kN and 69 kN, respectively. Figure 9 shows the morphology of a compressed specimen with a capsule of GPPS, ABS, and HIPS, respectively. It can be seen that the HIPS capsule ruptured, while GPPS and ABS capsules remained intact under loading.

Shear test of specimens

The shear tests of specimens were carried out. The

Fig. 10. Specimens with two capsules embedded for shear test.

Fig. 11. Shear test of a mortar specimen.

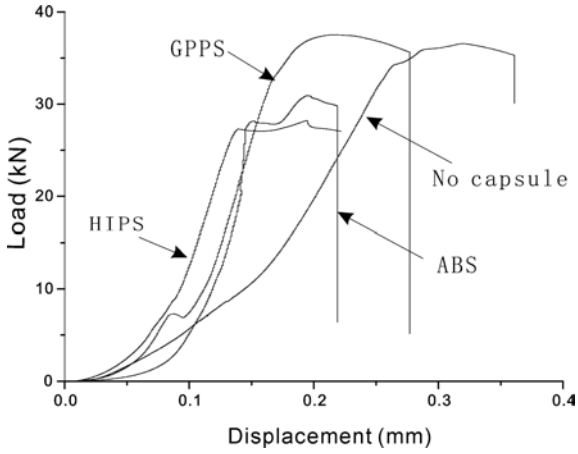

Fig. 12. Shear of specimen with a capsule.

cement mortar prismatic specimens were $40 \times 40 \times 160$ mm^3, in which two capsules were located at the boundary position of the upper loading head, as shown in Figure 10. The mix proportion was the same as that for compression test. The experimental set up was designed so that the lower supports which were 40 mm long on each side would just be contiguous to the upper loading head, as shown in Figure 11. The loading scheme was the same as that for the compression test.

The load-displacement curves for shear test of specimens with two capsules (GPPS, ABS, HIPS) and no capsule are shown in Figure 12. It was found the strengths for the specimens had similar trend with that of compression tests, that was GPPS and no capsule had higher values, whereas ABS and HIPS had similar lower values. The presence of capsules made the specimen more brittle than that without a capsule. Figures 13 and 14 show the morphology of a sheared specimen with a ruptured capsule and an intact capsule, respectively. It was also found that, similar to the compression test results, the GPPS and ABS capsules almost remained intact during the tests, while a large portion of HIPS capsules were ruptured. In both compression and shear tests, it was found that the capsules may either be ruptured or be debonded from the matrix materials. The self-healing function is based on the rupture of microcapsules. Thus determination of judgment criterion theoretically that under what condition a microcapsule ruptures is necessary.

Fig. 13. Morphology of a sheared specimen with a ruptured capsule.

Fig. 14. Morphology of a sheared specimen with an intact capsule.

Numerical Study on Interaction of a Microcapsule and a Crack

In this section, a numerical model, as depicted in Figure 15, was setup to investigate the interaction of a microcapsule and a crack using finite element package Abaqus [1].

First, for simplicity, a two-dimensional plane square area was considered, in which the side length was 10 mm. A microcapsule of radius 0.1 mm was located at the center of the area. Left hand side was laid a line crack. A Cartesian coordinate system of origin at the center of the microcapsule was setup, whereas the x-axis pointed toward right and the y-axis toward up. The

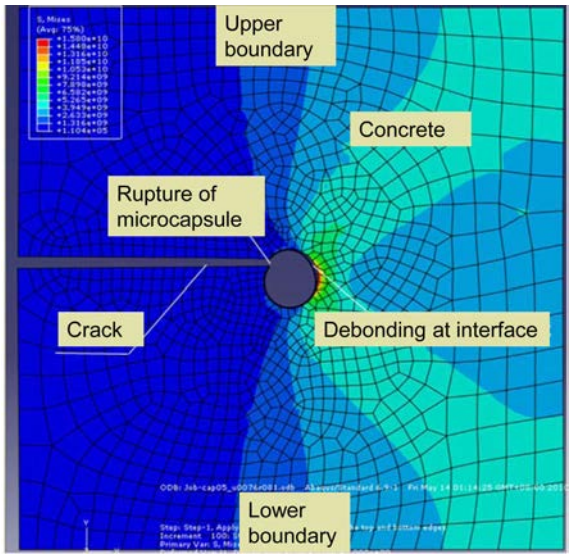

Fig.13. Computing model for a crack approaching a microcapsule.

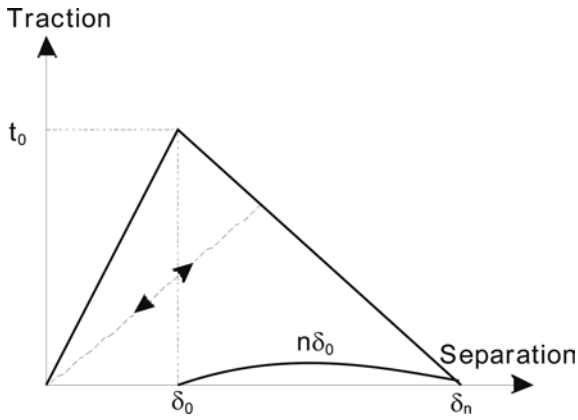

Fig. 14. Traction-separation relationship.

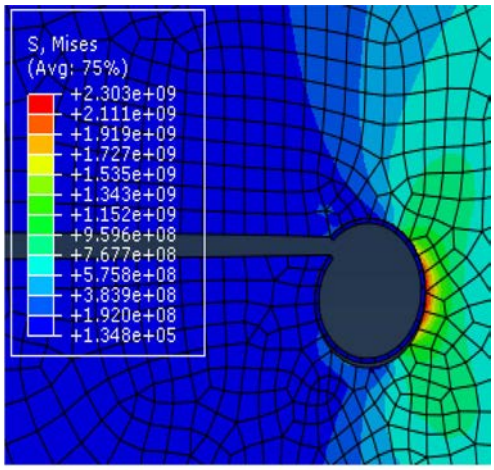

(a) Rupture of the microcapsule

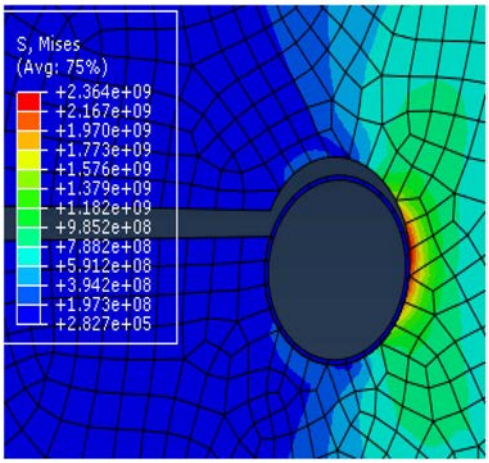

(b) Debonding of the microcapsule

Fig. 15. Status of a microcapsule when a crack approaches.

load was applied by using a small relative tensional displacement between upper and lower outer boundaries. A range of microcapsule thickness was considered from 0.003 mm to 0.008 mm. The possible fracture point of the microcapsule was supposed located near the crack tip. The rest area of the mortar matrix and the microcapsule was supposed elastic.

The interface between the microcapsule and the mortar matrix, as well as the bonding behavior of the microcapsule shell wall was modeled using the cohesive traction-separation constitutive relationship as shown in Figure 14, and following equation

$$t = K\delta \tag{2}$$

where t denotes the stress, δ represents the displacement separation, K is the stiffness matrix. In Equation (2), damage was considered. The damage initiation was dependent on the maximum stress criterion. The damage variable D monotonically evolves from 0 to 1 upon further loading after the initiation of damage. The contact stress components were affected by the damage according to

$$\begin{cases} t = (1-D)\tilde{t} & \text{tension and shear} \\ t = \tilde{t} & \text{for compression} \end{cases} \tag{3}$$

where $\tilde{t}$ is the contact stress components predicted by the elastic traction-separation behavior for the separations without damage. The damage evolution was based on the fracture energy, which denotes the area under the traction-separation curve.

From Figure 14, we know the fracture energy can be expressed as

$$G = \frac{1}{2}\delta_0 t_0 + \frac{1}{2} n\delta_0 t_0 = \frac{1}{2}(n+1)\delta_0 t_0 \tag{4}$$

Then δ_0 can be determined as

$$\delta_0 = \frac{2G}{t_0(n+1)} \tag{5}$$

The stiffness K was then determined based on fracture energy by

Table 2. Microcapsule rupture status under combination of parameters.

No.	Tensile strength of microcapsule wall	Tensile strength of the interface	Strength of microcapsule wall K_C / Strength of the interface K_D	Pattern: microcapsule ruptured / debonded
1	92e + 6	2.07e + 6	44	ruptured
2	56e + 6	2.07e + 6	27	ruptured
3	92e + 6	2.07e + 6	44	debonded
4	56e + 6	2.07e + 6	27	ruptured
5	92e + 6	2.07e + 6	44	ruptured
6	56e + 6	2.07e + 6	27	ruptured
7	92e + 6	2.07e + 6	44	ruptured
8	56e + 6	2.07e + 6	27	debonded
9	92e + 6	0.51e + 6	180.	debonded
10	56e + 6	0.51e + 6	110	debonded
11	92e + 6	0.51e + 6	180	debonded
12	56e + 6	0.51e + 6	110	debonded
13	92e + 6	0.51e + 6	180	debonded
14	56e + 6	0.51e + 6	110	debonded
15	92e + 6	0.51e + 6	180	debonded
16	56e + 6	0.51e + 6	110	debonded

$$K_0 = tan\theta = \frac{t_0}{\delta_0} = \frac{t_0^2(n+1)}{2G} \tag{6}$$

Here, to investigate the microcapsule rupture or debonding behavior, the related parameters were to be figured out, i.e. the strength of microcapsule wall K_C, the bonding strength between microcapsule and concrete K_D, the thickness of microcapsule wall, direction of the crack approaching the microcapsule (coordinate height h of the crack).

From the literature [25, 27, 28], we have known the range of the above parameters, for the microcapsule wall: Fracture energy: 8.0 ~ 12.9 N/m; wall strength, normal: 56 ~ 92 MPa, shear: 2.8 ~ 4.8 MPa. For the interface between mortar matrix and the microcapsule: strength was supposed half of the mortar strength: normal: 0.51 ~ 2.07 MPa shear: 0.45 ~ 2.05 MPa. Then fracture energy can be calculated from strength intensity factors (SIF) as $G = K^2 / E$.

Table 2 shows the failure patterns of a microcapsule under the combination of parameters of upper and lower bounds. It was found that in the all 16 cases (strength and fracture energy of microcapsule wall and the interface), a microcapsule would be ruptured in 6 cases whereas it would be debonded in 10 cases. Figure 15 shows the computing results for the possible patterns when a crack approached a microcapsule.

It is known a microcapsule could behave in two patterns (ruptured or debonded), and it is necessary to determine the criterion to make a judgment. We have known that if only rupture condition was considered, a microcapsule would be ruptured when $\sigma_C = K_C$, i.e. the effective stress reached its strength. The equation could be rearranged to $\sigma_C/K_C = 1$; if only interface condition was considered, an interface would be debonded when $\sigma_D = K_D$, i.e. the interface effective stress reached its strength, which was rearranged to $\sigma_D/K_D = 1$. When the two cases were possible to occur, we should compare the values σ_C/K_C and σ_D/K_D. A microcapsule would be ruptured if $\sigma_C/\sigma_C > K_D/K_D$, which could be rearranged to $\sigma_C/\sigma_D > K_C/K_D$ provided all factors were positive values; otherwise, the microcapsule would be debonded. Thus a function could be defined as follows:

$$Q = \frac{\sigma_C}{\sigma_D} - \frac{K_C}{K_D} \begin{cases} >0 \text{ Microcapsule rupture} \\ <0 \text{ Microcapsule debonding} \\ =0 \text{ limiting state} \end{cases} \tag{7}$$

Here, the limiting state was defined that, the point was obtained when one of the parameters varies a small value, the failure pattern changed from microcapsule rupture to debonding or from debonding to rupture. It was clear that σ_C/K_C should be a function of geometric parameters in elastic state for particular loading. Thus we have

$$\frac{\sigma_C}{\sigma_D} = F\left(\frac{t}{R}, \frac{h}{R}\right) \tag{8}$$

Then the criterion for a capsule rupture or debonding could be expressed in terms of three normalized parameters t/R, h/R, and K_C/K_D:

$$Q = F\left(\frac{t}{R}, \frac{h}{R}\right) - \frac{K_C}{K_D} \tag{9}$$

where R and t represent the outer radius and the thickness of the microcapsule, respectively; h denotes the height coordinate of the crack. By using the above model, varying t/R from 0.01 to 0.08, and h/R from 0.2 to 0.8, forty limiting state points were obtained as shown in Figure 16. Each point represented a limiting state of a combination of the parameters, which was obtained by trial-and-error procedure. It could be seen from the figure that the values of K_C/K_D were located from 39.0 to 90.0.

In order to make use of the results, these forty points need to be regressed to a surface. Through a variety of tests using Matlab, the following polynomial of 4th power led to relatively satisfactory results.

$$\begin{aligned} Q &= F\left(\frac{t}{R}, \frac{h}{R}\right) - \frac{K_C}{K_D} \\ &= 110.8 + 539.5\left(\frac{h}{R}\right) - 5438\left(\frac{t}{R}\right) - 1774\left(\frac{h}{R}\right)^2 \\ &\quad - 1823\left(\frac{h}{R}\right)\left(\frac{t}{R}\right) + 159900\left(\frac{t}{R}\right)^2 + 1701\left(\frac{h}{R}\right)^3 + \\ &\quad 26810\left(\frac{h}{R}\right)^2\left(\frac{t}{R}\right) - 249100\left(\frac{h}{R}\right)\left(\frac{t}{R}\right)^2 - 1296000\left(\frac{t}{R}\right)^3 \\ &\quad - 419.8\left(\frac{t}{R}\right)^4 - 23770\left(\frac{h}{R}\right)^3\left(\frac{t}{R}\right) + 116000\left(\frac{h}{R}\right)^2\left(\frac{t}{R}\right)^2 \\ &\quad + 957100\left(\frac{h}{R}\right)\left(\frac{t}{R}\right)^2 + 3252000\left(\frac{t}{R}\right)^4 - \frac{K_C}{K_D} \end{aligned} \tag{10}$$

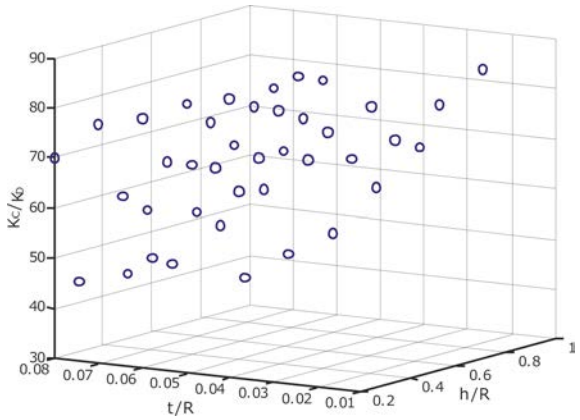

Fig. 16. Points at limiting state.

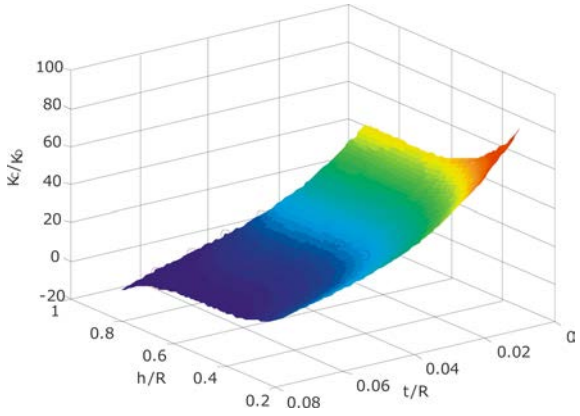

Fig. 17. Criterion surface for determination of a microcapsule rupture or debonding.

The goodness of the regression was: SSE (Sum squared error) = 139.4; R-square = 0.9831, which R-square was the square of the correlation between the response values and the predicted response values. Adjusted R-square = 0.9737; RMSE (root mean square prediction error) = 2.362. The polynomial could be depicted as a surface shown in Figure 17, where a point under the surface means $Q > 0$, corresponds to that a microcapsule ruptures, otherwise, the microcapsule is debonded. With this criterion, we can judge a microcapsule behavior using the parameters without need of FEM computation every time.

Summary and Conclusions

(1) In this study, a macro capsule model experiment was developed to simulate the microcapsule behavior in cementitious materials. In compression and shear tests, both rupture and debonding pattern of capsules were observed.

(2) A criterion for judgment of a microcapsule rupture or debonding when a crack approach was obtained. With this criterion, one can determine a microcapsule behavior using the parameters without computation every time.

(3) It is expected to further investigate the mechanism of self-healing process theoretically in future.

Acknowledgments

The authors would like to acknowledge financial support provided by International Cooperation and Exchange of the National Natural Science Foundation of China (No. 51120185002), Collaborative Innovation Center for Advanced Civil Engineering Materials, Nanjing, P.R. China; The General Program of National Natural Science Foundation of China (51478272). Joint funds of the National Natural Science Foundation of China and Guangdong Province (U1301241), the Science and Technology Foundation for Basic Research Plan of Shenzhen City (JCYJ20140418 182819159).

References

1. *ABAQUS/Standard User's Manual*, ver. 6.9, 2009. Simulia.
2. Ahn, T.H. & Kishi, T. 2010. Crack self-healing behavior of cementitious composites incorporating various miner admixtures. *J. Adv. Concr. Technol.* 8:171-186.
3. Brady, G.S., Clauser, H.R., Vaccari, J.A., 2002. *Materials Handbook (15th ed.)*. New York, NY: McGraw-Hill.
4. De Rooij M., Van Tittelboom K., De Belie N, & Schlangen E (eds.) 2013. Self-Healing Phenomena in Cement-Based Materials, *State-of-the-Art Report of RILEM Technical Committee 221-SHC*, Dordrecht: Springer.
5. Dry, C. & McMillan, W. 1996. Three-part methylmethacrylate adhesive system as an internal delivery system for smart responsive concrete. *Smart Mater. Struct.* 5:297-300.
6. Dry, C.M. 2000. Three designs for the internal release of sealants, adhesives, and waterproofing chemicals into concrete to reduce permeability. *Cem. Concr. Res.* 30: 1969-1977.
7. Igarashi, S, Kunieda, M. Nishiwaki, T., 2009. Autogenous-healing in cementitious materials. *Technical Committee Report of JCI-TC075 B*: 91-102. Japan Concrete Institute.
8. Jefferson, A., Joseph, C., Lark, R., Isaacs, B., Dunn, S.C., Weager, B. 2010. A new system for crack closure of cementitious materials using shrinkable polymers. *Cem. Concr. Res.* 40:795-801.
9. Jonkers, H.M. 2007. Self-healing concrete: A biological approach. In *Self Healing Materials: An Introduction*; van der Zwaag, S., (Ed.), Springer: Dordrecht, The Netherlands, 195-204.
10. Jonkers, H.M., Thijssen, A., Muyzer, G., Copuroglu, O., Schlangen, E. 2010. Application of bacteria as self-healing agent for the development of sustainable concrete. *Ecol. Eng*. 36:230-235.
11. Joseph, C., Gardner, D., Jefferson, T., Isaacs, B., Lark, B. 2010. Self-healing cementitious materials: A review of recent work. *Proc. ICE Constr. Mater.* 164:29-41.
12. Keller M.W. & Sottos N.R. 2006. Mechanical properties of microcapsules used in a self-healing polymer. *Experimental Mechanics* 46:725-733.
13. Kishi, T., Ahn, T.H., Hosoda, A., Takaoka, H. 2007. Self-healing behavior by cementitious recrystallization of cracked concrete incorporating expansive agent. In *Proceedings of the First International Conference on Self-Healing Materials*, Noordwijk, The Netherlands, 18-20.
14. Li, V.C., Lim, Y.M., Chan, Y.W. 1998. Feasibility study of

a passive smart self-healing cementitious composite. *Compos. B* 29:819-827.
15. Mihashi, H.; Nishiwaki, T. 2012. Development of engineered self-healing and self-repairing concrete-state-of-the-art report. *J. Adv. Concr. Technol.* 10:170-184.
16. Mihashi, H., Kaneko, Y., Nishiwaki, T., Otsuka, K. 2000. Fundamental study on development of intelligent concrete characterized by self-healing capability for strength. *Trans. Jpn. Concr. Inst.* 22:441-450.
17. Nishiwaki, T., Mihashi, H., Jang, B.K., Miura, K. 2006. Development of self-healing system for concrete with selective heating around crack. *J. Adv. Concr. Technol.* 4: 267-275.
18. *Proceedings of 4th international conference on self-healing materials*, 2013. (ed.), N. De Belie, S. van der Zwaag, E. Gruyaert, K. V. Tittelboom, B. Debbaut, Publisher: Magnel Laboratory for Concrete Research, Technologiepark Zwijnaarde 904, 9052 Ghent, Belgium.
19. Sakai, Y., Kitagawa, Y., Fukuta, T., Iiba, M. 2003. Experimental study on enhancement of self-restoration of concrete beams using SMA wire. *Proc. SPIE* 5057:178-186.
20. Tittelboom K.V. & De Belie N., 2013. Self-healing in cementitious materials-a review, *Materials* 6:2182-2217.
21. Tittelboom, K.V., Belie, N.D., Muynck, W.D., Verstraete, W. 2010. Use of bacteria to repair cracks in concrete. *Cem. Concr. Res.* 40:157-166.
22. Wang, X.F., Xing, F., Zhang, M., Han, N.X. & Qian, Z. 2013. Experimental study on cementitious composites embedded with organic microcapsules, *Materials* 6, 4064-4081.
23. White, S.R., Sottos, N.R., Geubelle, P.H., Moore, J.S., Kessler, M.R., Sriram, S.R., Brown E.N., Viswanathan, S. 2001. Autonomic healing of polymer composites. *Nature* 409:794-797.
24. Wu, M., Johannesson, B., Geiker, M. 2012. A review: self-healing in cementitious materials and engineered cementitious composite as a self-healing material. *Constr. Build. Mater.* 28:571-583.
25. Wu, Z. M., Zhao, G. F., Huang, C. 1993. Fracture toughness and fracture energy for different concrete strength. *Journal of Dalian University of Technology* 33(S1):73-77.
26. Xing, F. Ni, Z. Han, N. Dong, B. Du, X. Huang, Z. Zhang, M. 2008. Self-Healing mechanism of a novel cementitious composite using microcapsules. In *Proceedings of the International Conference on Durability of Concrete Structures*, Hangzhou, China, 26-27.
27. Yang, Y. J. 2007. Research on fracture of microcapsule based self-healing materials. *Master thesis, Zhengzhou University*, Hangzhou, China.
28. Zhao, Q. S. 2003. *Advanced Handbook of Composite Materials*, China Machine Press.